AIAA 2000-0826
Rapid Model Fabrication and Testing for Aerospace Vehicles

G. M. Buck
NASA Langley Research Center
Hampton, VA

38th Aerospace Sciences Meeting & Exhibit
10-13 January 2000
Reno, Nevada

2000-0826

RAPID MODEL FABRICATION AND TESTING FOR AEROSPACE VEHICLES

Gregory M. Buck*
NASA Langley Research Center
Hampton, VA 23681-2199

Abstract

Advanced methods for rapid fabrication and instrumentation of hypersonic wind tunnel models are being developed and evaluated at NASA Langley Research Center. Rapid aeroheating model fabrication and measurement techniques using investment casting of ceramic test models and thermographic phosphors are reviewed. More accurate model casting techniques for fabrication of benchmark metal and ceramic test models are being developed using a combination of rapid prototype patterns and investment casting. White light optical scanning is used for coordinate measurements to evaluate the fabrication process and verify model accuracy to ±0.002 inches. Higher-temperature (<210C) luminescent coatings are also being developed for simultaneous pressure and temperature mapping, providing global pressure as well as global aeroheating measurements. Together these techniques will provide a more rapid and complete experimental aerodynamic and aerothermodynamic database for future aerospace vehicles.

Introduction

Aerothermodynamics, combining aerodynamic, aeroheating and fluid dynamic measurements and predictions, forms the core discipline for the design, development and flight of aerospace vehicles such as space transportation vehicles, planetary probes, and Earth return vehicles.

Flight simulation via ground-based hypersonic facilities have been tried and proven for over 40 years and today, for a given time interval, wind tunnels can provide orders of magnitude more aerothermodynamic information than computational methods. This is particularly true for advanced aerospace vehicles having complex geometries such as X-33, X-34 and Hyper-X (e.g., vehicles having fins, control surfaces, inlets, nozzles, etc.) as opposed to more simple reentry capsules and aerobrakes.

The present challenge for experimental testing is to reduce the wind tunnel test cycle (the elapsed time from the receipt of the vehicle coordinates to delivery of the test data to the customer), particularly the model fabrication time which now accounts for roughly 70% of the total test cycle. Presently, it takes several months to design, fabricate and test a single metallic force and moment wind tunnel test model for heated hypersonic wind tunnels. To reduce this time to weeks, even days, will require a revolutionary change in the way models are fabricated and tested.

Dimensional accuracy (e.g., outer mold line fidelity, balance position, fitting tolerance), surface finish and material strength are important requirements in the design and construction of wind tunnel test models. These requirements vary according to the experimental facility, measurement technique and experiment objectives. Smaller facilities and test models generally require higher accuracy for flight simulation. So do benchmark aerodynamic studies for flight readiness or quantitative aeroheating measurements for optimizing a thermal protection system. Fitting and re-fitting model parts for configuration build-up studies requires high accuracy in small detail so that parts fit the first time between tunnel runs. Boundary layer transition studies require smooth surface finishes. Aerodynamic models tested in the Langley Aerothermodynamics Facilities Complex are exposed to the flow for several minutes and have to be more durable than transient aeroheating test models. The model requirements (i.e., accuracy, finish and material strength) determine the usefulness for any given rapid fabrication technique.

*Aerospace Technologist, Aerothermodynamics Branch, Aerodynamics, Aerothermodynamics and Acoustics Competency

In the late 1980s, machine tools were used at NASA Langley for the National Aero-Space Plane (NASP) development. Coordinates for configuration 201 were electronically transferred to Langley, immediately loaded onto machine tools, and models fabricated in a fast-paced manner without formal model design. High fidelity, complex configuration steel models were fabricated for force and moment and for pressure testing. Ceramic aeroheating models were made for thermal mapping studies. Ceramic models were also instrumented with thin film gages for quantitative aeroheating measurements. These models were constructed, tested and the data reduced, analyzed, and disseminated within a matter of months. (Miller, 1998)

The fast paced machining methods demonstrated for the NASP program can, in reality, be maintained only for relatively short periods of time and requires high Center priority, as machine space is limited and personnel intensive. For NASP, machines were run on overtime, day and night, and many personnel were required.

To technically improve machining capability, Langley is acquiring high-speed machine tools for fabrication of soft metals such as aluminum, higher strength steels (e.g., 15-5 PH stainless) and possibly ceramics. These tools will significantly reduce the time it takes to fabricate a test model by both removing material more quickly from a machined surface and reducing time in hand working by producing smoother surfaces. Tighter tolerances (± 0.0005 versus ± 0.005 with current technology) also mean less time involved in assembly, working and fitting parts together. Langley is also forming alliances with other national laboratories and industry to develop direct metal fabrication of lightweight aerodynamic structures and wind tunnel models using laser light fabrication techniques. This revolutionary technique may have several applications, particularly for very high strength steels (e.g., Vascomax 200) used in high Reynolds number facilities such as the National Transonic Facility at Langley.

Commercial rapid prototyping techniques such as stereolithography resin have been used extensively at Langley to fabricate complex configurations in one to two days time. Many models have been fabricated and tested directly with stereolithography for aerodynamic screening studies in the 22-Inch Mach 20 Helium Tunnel (Miller, 1998) with unheated flows and model surface temperatures at or below room temperature. Fused deposition and layered object manufacturing techniques have been used at Marshall Space Flight Center (Springer, 1998) in unheated flows. A useful evaluation of many of these techniques for wind tunnel model fabrication was made recently by Chuk and Thomson, 1998, in the Rapid Prototyping Journal.

Casting techniques have been used generally to reduce fabrication time for metals and ceramics, particularly for screening studies, where high accuracy is not required. Casting is inherently fast once the process is in place and the molds are formed. Casting has the added advantage that production can be increased for a given time interval by pouring several models at one time. Rapid prototyping techniques increase the speed and applicability of casting with complex patterns and mold forming. Production of stereolithography patterns, like castings, can be increased for a given time interval by building several patterns in a batch at one time.

Advances have been made in global measurement techniques for pressure, temperature and transient heat transfer measurements on wind tunnel models. These techniques revolutionize wind tunnel testing by providing high resolution surface measurements in very little time with low cost. Pressure- and temperature-sensitive paints have been developed for several applications in subsonic through supersonic conditions, with some low temperature hypersonic applications (Liu, et al., 1997). Two-color thermographic phosphors have been developed for higher temperature hypersonic wind tunnels for surface temperature and transient heat transfer measurements (Merski, 1999), and pressure-sensitive coatings are being developed at present for pressure measurements in heated hypersonic facilities.

This paper will review global aeroheating test methods and rapid casting techniques for ceramics and metals and describe efforts made in making casting techniques more accurate and developing higher temperature pressure and temperature sensitive coatings for better and faster aerothermodynamic measurements.

Background

Rapid Model Fabrication and Testing for Aeroheating Measurements

Quantitative aeroheating test methods at Langley from the early 1980s until the early 90s required models with machined ceramic inserts and thin film gages. (Schultz and Jones, 1973, Miller, 1981, 1984.) In the late 1980s and early 90s, a typical thin film aeroheating test model with 150 to 250 gages would take a year to fabricate and cost up to $150K. Fast paced programs such as the National AeroSpace Plane and Personnel Launch System, HL-20, required more rapid techniques. With thin film technology, quantitative aeroheating data could not be produced fast enough to

Table 1. - Typical Quantitative Aeroheating Experiment Before and After Phosphor Thermography.*

	Better	Faster	Cheaper
Before	Discrete gages 150 points/run	50 weeks to obtain data on study	Fabrication cost: $150K (1 model)
After	Global data 150,000 points/run	5 weeks to obtain data on study	Fabrication cost: $15K (5 models)
Impact to a study	Increased amount of Information: **1000x**	Time savings: **10x**	Cost reduction: **10x**

*Miller, 1998.

be included in the fast paced design cycle. Experimental aerodynamic force and moment data could be acquired in a few months time and used to modify outer mold lines to enhance aerodynamic performance before the first experimental heating data was produced. With this scenario, the aeroheating test model was obsolete before it was ever tested.

Global aeroheating test methods were then developed using slip cast ceramic test models and quantitative thermal imaging techniques to reduce model fabrication and test time. With this test method the sequence of acquiring aerodynamic and aeroheating test data was reversed. A patented investment technique for ceramic slip casting (Buck and Vasquez, 1989) allowed the creation of complex models having thin sections such as wings or fins in a matter of days. Two-color thermographic phosphor coatings and image acquisition systems (Buck, 1988, 1989) replaced the thin film heat transfer gages. User friendly tools to view and analyze the data (Merski, 1998) and an improved temperature calibration technique (Merski, 1999) improved the method even further.

Experimental aeroheating information now precedes experimental aerodynamic information in hypersonics and is an integral part of early aerospace vehicle design.

Test Model Requirements

Model requirements are generally determined by the test facilities, a tabulation of model requirements for Langley by facilities is listed in Table 2. The typical range in tolerance, or outer mold line fidelity, was determined by typical fabrication requests and not necessarily the model scale or test objectives. Requested tolerance is frequently affected by budget and time constraints. For example, a 0.003 inch tolerance stainless steel model will cost significantly more to have machined than a 0.005 inch tolerance model, and take twice as long to fabricate. Ultimate tensile strength (UTS) requirements are less subjective. UTS is directly a function of dynamic pressure (q), model geometry and attitude.

Models tested in hypersonic facilities fall within the moderate to low strength requirements (14-68 ksi). The strength of cast metals, even the lower temperature melting brass and aluminum alloys, are generally high

Table 2. - Aerodynamic Model Requirements by Langley Facility.*

	q(psi)	Service Temp. (F)		Test Core (in.)		UTS (ksi)	Tolerance (Typical)	
Facility	max.	min.	max.	width	height	max.	min.(in)	max.(in.)
20-Inch M 6 Air Tunnel	7.5	408	476	14	14	68	0.003	0.005
31-Inch M10 Air Tunnel	2.4	1340	1365	12	12	22	0.003	0.005
20-Inch M 6 CF4 Tunnel	1.6	664	708	14	14	15	0.003	0.005
22-Inch M 20 He Tunnel	4.3	68	68	12	12	39	0.003	0.005
Unitary Plan Tunnel	19	100	300	48	48	167	0.003	0.010
National Transonic Fac.	22	-250	120	98	98	200	0.001	0.005
14x 22-Ft. Subsonic Tun.	1.4	0	160	174	261	13	0.005	0.030
8-Ft. High Temp. Tunnel	22	1640	3650	96	96	194	0.005	0.015

*figures prepared by T. Biess

enough for testing in these facilities. The lower melting temperature alloys can also be cast with more accuracy, smoother surfaces and finer details than the higher strength and higher melting temperature steels and nickel alloys.

Development of More Accurate Rapid Casting Techniques

White Light Optical Coordinate Scanner

For evaluation of the different casting techniques a non-contact white light optical coordinate scanner is used. Unlike conventional coordinate measurement machines, the non-contact white light scanner can provide global model coordinate data in a matter of hours. With this scanner, patterns, molds, cast wax investment patterns, rapid prototype investment patterns and castings can be accurately and completely scanned, providing a means not only for final model verification, but process control.

This system measures objects at high data density (approximately 400,000 object pixels per image) and offers them as point clouds for reprocessing or visual inspection.

Various fringe patterns are projected onto the object's surface and grabbed by two cameras from different angles (figures 1 and 2). With digital image processing and based on the principle of triangulation, the three-dimensional coordinates are computed independently with high accuracy for as many as 400,000 camera pixels per scan. If the object is moved or shadows cast on the surface from another source during a scan session, analysis software is programmed to detect the error between scans so that the scan can be discarded or affected areas removed from the final result. Different lens sets provide sample measurement volumes of 3-inch squared with $\pm$ 0.001 inch accuracy, 6-inch squared with $\pm$ 0.002 inch accuracy, and 11-inch squared with $\pm$ 0.003 inch accuracy.

Each scan takes approximately 30 seconds to complete. Multiple scans are automatically aligned together as the object is scanned using targets placed on the object and/or in the scene. Very large objects can be scanned accurately using typical photogrammetry to find the coordinates of all of the targets around and on the object and the white light optical scanner to fill in the surface coordinates. A typical scanning session on a 10 inch long test model takes 4 hours with approximately 1 million object pixels on the surface using the medium sized lens set with $\pm$0.002 inch accuracy.

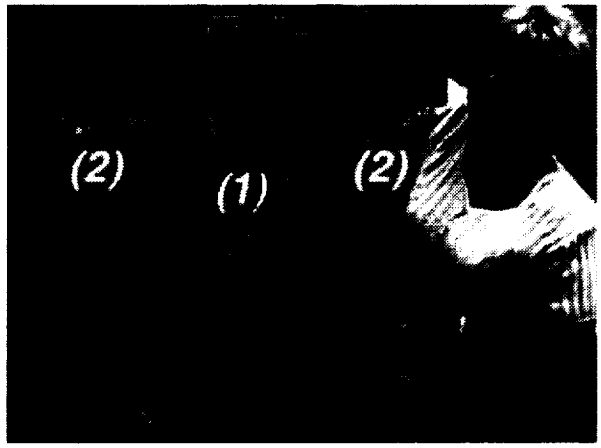

Figure 1. - White light optical coordinate scanner, (1) projector and (2) two image sensors.

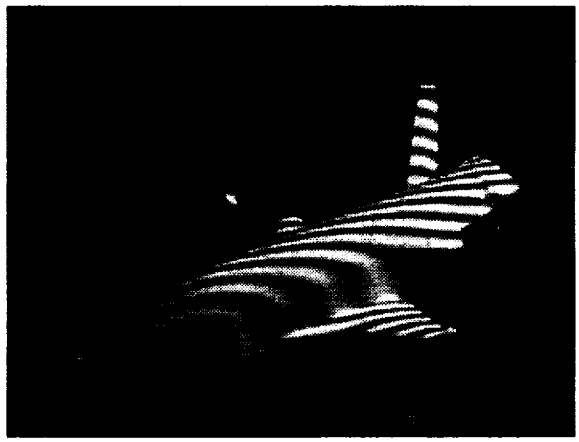

Figure 2. - Fringe patterns projected on model surface.

Slip Cast Silica Ceramic

Slip casting is a low cost, room temperature, atmospheric pressure, powder forming process typically used for fabricating ceramics. A "slip" refers to a crowded suspension of particles in a liquid. In the process of slip casting the slip is poured into a porous or liquid permeable mold, such as plaster of Paris used with aqueous or water based slips. The mold draws liquid from the slip compacting the powder along the mold surface to form a high-density cast shape. This cast shape is referred to as being in the "green" state. This state has to have some strength so that the mold can then be removed. Intermediate binders are usually added to the slip to give it this green strength. After removal from the mold, it is taken to a high temperature (2150°F for silica ceramic) burning out the intermediate binder and bonding, or "sintering," the powder to itself

forming a high purity material and giving it its final strength. Conventional molds (as shown in Figure 3) used to cast early models were multi-part plaster molds similar to those used in industry for producing sanitary ware, plates and pottery, foundry troughs, and electronic insulators.

Early use of slip casting in fabrication of aeroheating wind tunnel test models is documented in a NASA contract report (Dean and Connor, 1972), with typical fabrication procedures.

Advantages of the slip cast process include hollow, thin walled castings, high purity materials, void free substrates, smoothness and an accurate reproduction of the mold surface. Accuracy is achieved because of the low shrinkage of the ceramic during drying and sintering. The silica slip used for aeroheating test models is 83% solids and the slip casting process removes most of the remaining liquid to compact the green shape. Silica ceramic also has very low linear shrinkage relative to other ceramic slip castings. With complete sintering from a fully dense casting, silica has a theoretical minimum shrinkage of 0.75%, whereas alumina ceramic has a theoretical minimum linear shrinkage of 3%.

Model supports are mounted with a second backfill ceramic. Since the natural fabrication of the slip cast ceramic leaves a center cavity, the support hardware can be freely positioned and cemented in place as shown in Figures 4 and 5. A fixture can be accurately aligned using the original pattern. After mounting, an aeroheating test model is then coated with thermographic phosphors and tested.

Model supports, or "stings," are generally steel rods, sometimes hollow for carrying instrument wiring or pressure tubes. For larger models, flanges on the sting are required to restrict movement or prevent

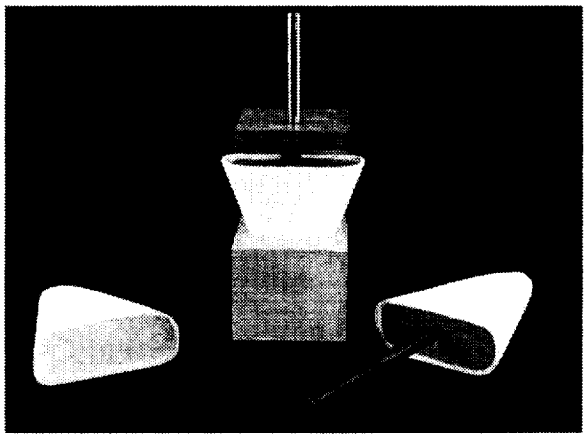

Fig.ure 4. - Fixture for sting mounting

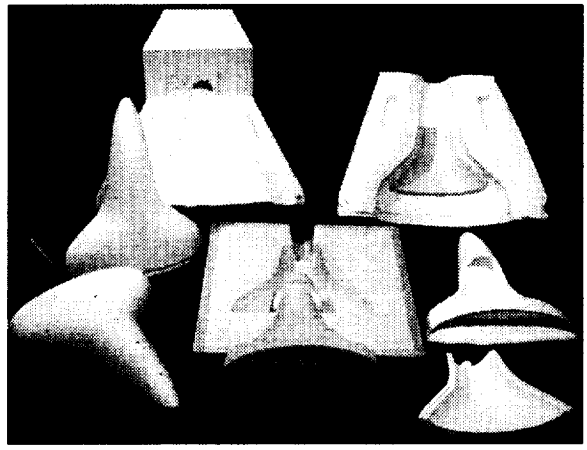

Figure 3. - Conventional plaster slip molds and castings (1989).

release from the backfill. Force and moment models are backfilled with removable sleeves pinned on the sting or "dummy" balance, to be used later for mounting on a "live" balance in the wind tunnel. Models have been mounted with blade mounts to minimize base flow interference. (see figure 7) Composite materials with low thermal conductivity are also being developed for various model and support components to reduce heat conduction to force and moment balances.

A process was invented at Langley for slip casting using investment shell molds. (Buck and Vasquez, 1989) This technique provides greater detail in slip castings, facilitating castings with fins and wings attached and properly aligned and eliminating mold parting lines from leading edges. In place of a multi-part plaster mold a refractory reinforced slurry mixture is used to apply a shell mold to an investment pattern. This shell mold will sustain temperatures high enough to burn out the investment pattern and is softened when wetted, to be easily removed from delicate slip castings.

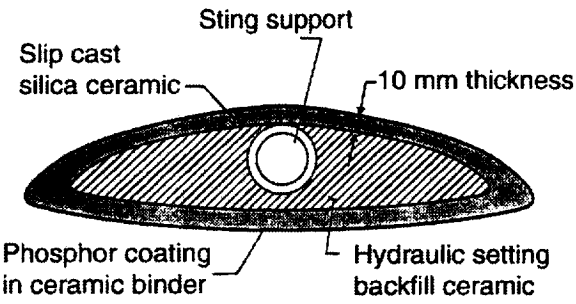

Figure 5. - Cross section diagram of typical mounted test model.

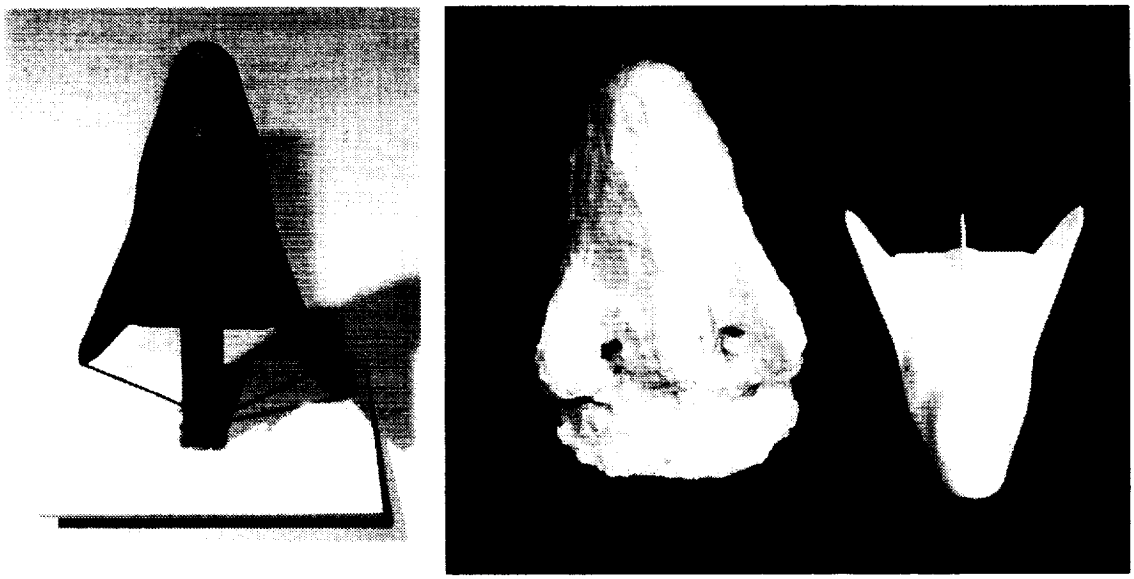

Figure 6. - Wax pattern, investment shell mold and slip cast ceramic HL-20 test model.

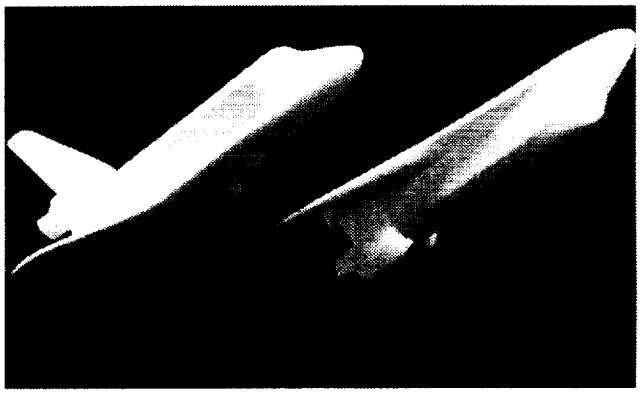

Figure 7. - Full configuration shuttle orbiter models.

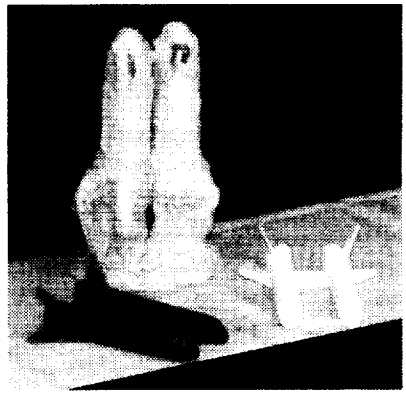

Figure 8. - Fly-back twin booster model.

Figure 6 shows a machined wax pattern, shell mold and slip cast nine-inch long ceramic test model of the NASA HL-20 orbital reentry lifting body. Figures 7 and 8 further demonstrate the wings, fins and leading edges made possible with investment shell molds and ceramic slip casting. Figure 7 is a full configuration shuttle orbiter test model and figure 8 a liquid fuel fly-back twin booster concept for replacing the shuttle solid rocket boosters.

Used together with rapid prototype patterns, the inexpensive production of net-cast shell molds for ceramic slip casting has produced hundreds of ceramic aerothermodynamic test models used in Langley hypersonic facilities for aeroheating and some force and moment measurements. (In X-33 Phase I studies at Langley, slip cast ceramic models were used for both aeroheating and force and moment testing.)

In figure 9, a 14-inch long slip cast ceramic

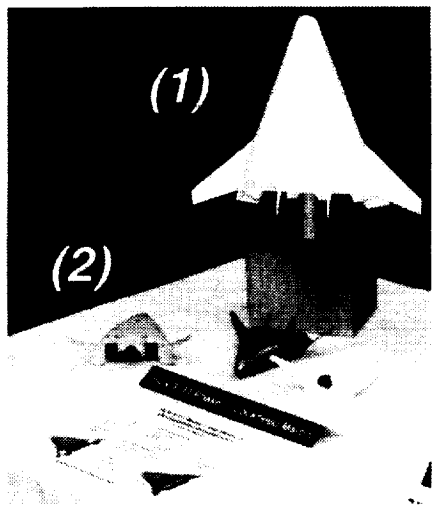

Figure 9. - X-33 Phase I test models.

phosphor aeroheating model and three 6-inch long force and moment models are shown. From left to right, the 6-inch models shown are a stereolithography resin model with steel balance sleeve, a cast steel blank and a slip cast ceramic model with steel balance sleeve. Stereolithography resin models are used in the unheated flow of the 22-Inch Mach 20 Helium Tunnel. Precision bore steel sleeves are fitted into the models for internal force and moment balance mounting.

White light optical scanning, as previously described, is being used to evaluate accuracy in the casting process and to develop new methods with higher accuracy. Digitized configurations are compared with original build files to provide useful accuracy images.

Figure 10 is a scan comparison for the bottom mold piece used in making wax model patterns for Future X Advanced Technology Vehicle, configuration H (X37H). (Note that tail fins are not included in this part of the mold or scan.) The scan comparisons are shown in a gray intensity scale from ± 0.035 inches. The scan in figure 11 is for a slip cast ceramic model using a wax pattern from the mold scanned in figure 10. Notice a similar pattern of deviations in the wing and nose area of both scans from the build file. In the ceramic casting, figure 11, the features are more prominent, indicating similar errors in both steps of the process, being additive in the result. In figure 12, a scanned ceramic casting from another configuration mold (X37G) shows a different pattern of deviations from the build file. It is expected that a careful evaluation of the similarites and differences in casting deviations such as these will be useful in developing a more accurate process downstream. At present, slip casting accuracy can be characterized as being within ± 0.040 inches.

A significant improvement in casting accuracy can be made with the implementation of a newer shell mold casting system developed at Langley, along with more accurate methods of forming investment patterns. As discussed previously, the actual slip casting replicates the mold surface with high accuracy. The development of rapid and accurate investment patterns will be discussed in a later section.

The newer shell casting system uses a multi-layer dipping process into alternating fine ceramic slurries and fluidized powders to form a more dimensionally stable shell mold for slip casting. The newer shell mold has less movement during the setting, drying and wax burn out processes. It also has improved slip casting properties, with more uniform and thinner shell walls which are easier to form and to later remove from difficult configurations, such as hollow cores, gaps between control surfaces and thin trailing edges.

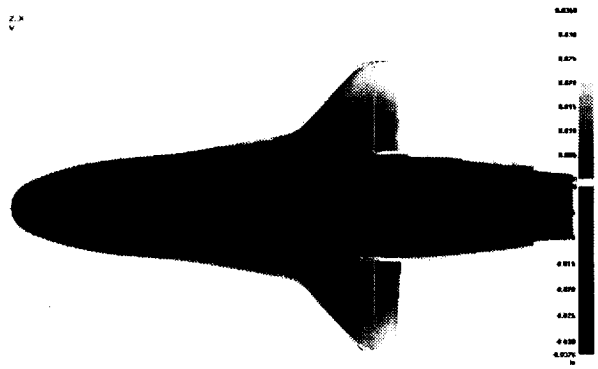

Figure 10. - Wax injection mold, X37H.

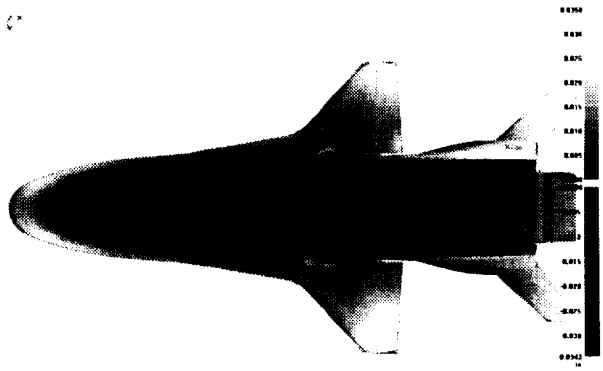

Fig.ure 11.- Cast ceramic, X37H.

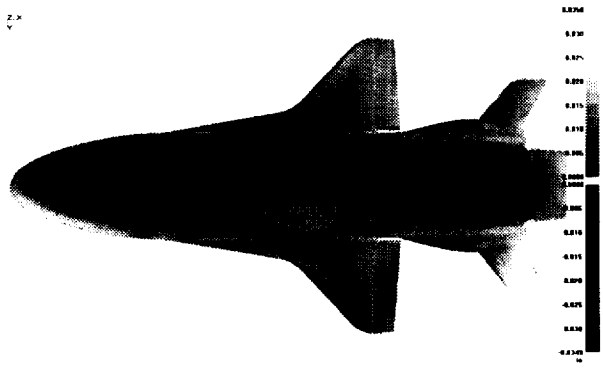

Figure 12. - Cast ceramic, X37G.

Table 3. - Slip-Cast Fused Silica (as cast)

	Linear change, %	Flatness, inches
Original Shell Slip Mold	+0.4050	-0.02682
Newer Shell Slip Mold	+0.0598	-0.00581

Table 4. - Hydraulic Setting Impression Molds (as cast)

	Linear change, %	Flatness, inches
Ceramacast 510	+0.0300	-0.00189
RS-17A Castable	+0.0232	+0.00760
RS-17E Castable	+0.0692	-0.00179

The newer shell mold casting system was evaluated prior to acquiring the white light scanning system and was evaluated using a coordinate measuring machine. Slip molds were first cast from a 12-inch calibration steel bar with markings 10-inches apart, known within ± 0.0001 inches. The original shell slip mold, formed on the bar by hand and trowel, and the newer shell slip mold, formed using a multi-layer dipping process were cast, fired and then used to slip cast a replica of the calibration steel bar in silica ceramic. Percent linear change and flatness measurements were then made with a touch trigger probe. Linear growth or shrinkage (+ or -) presented in tables 3 and 4 are given in percent change from the 10 inch markings on the original steel block.

Flatness is computed by subtracting the maximum of 24 points above and 24 points below a best-fit plane for the measured surface. Measured flatness values in tables 3 and 4 are given a + or - sign depending on the apparent bow direction relative to the original steel block. The original steel block surface flatness is measured at +0.00051 inches using the same method.

Improvements are shown to be 5 to 6 times the precision on linear growth and flatness over the original shell slip mold (table 3). The newer shell slip mold results are comparative with results obtained from impression molds using other hydraulic "cast-to-size" ceramics as shown in table 4. As this newer shell mold casting system is evaluated with hypersonic wind tunnel models it is expected that the slip casting accuracy will improve significantly.

Pressure Cast Aluminum

A pressure casting process for low melting temperature metals (<1800F) was developed for castings with fine features and thin sections. (Vasquez et al., 1989) This process also has potential for accurate model casting.

The process uses an injection rig with a vertical pneumatic piston and cylinder to inject molten metal into an investment mold at pressure. The mold canister is shown being positioned on the rig in figure 13a. The cylinder is lined and insulated with flexible ceramic felt as shown in figure 13b. The investment mold is cast into a reinforced metal canister (figure 13c) over a wax pattern. The mold is kept preheated in a gas furnace until assembly on the rig for casting. When the molten metal is at temperature for casting it is poured into

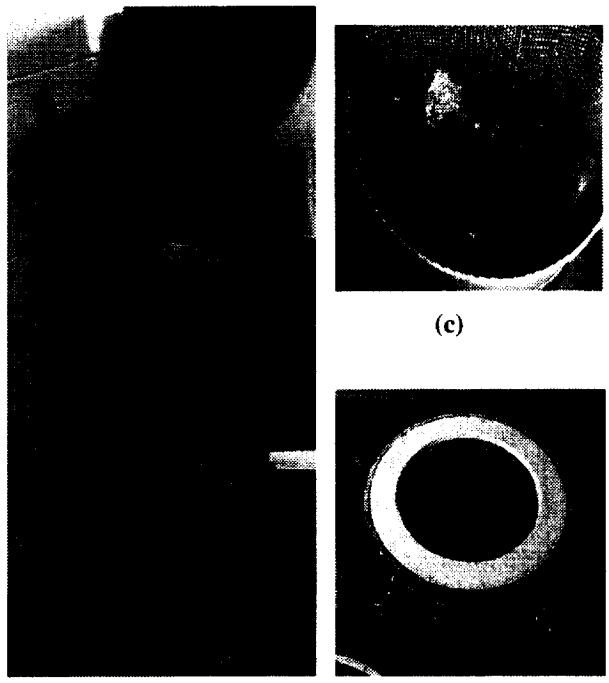

(a) (b) (c)

Figure 13. - Components of pressure casting process, (a) pressure casting rig, (b) insulated cylinder, (c) mold canister with wax pattern.

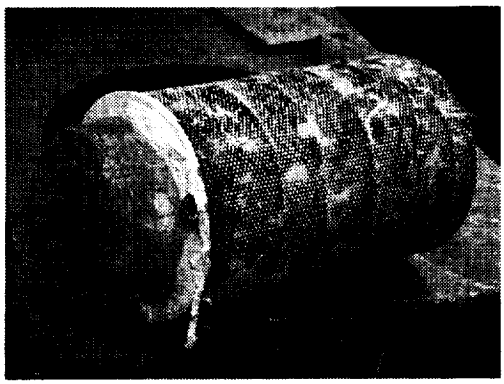

(d)

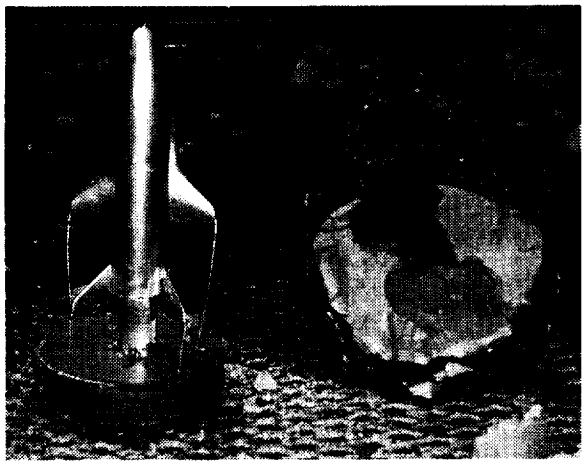

(e)

Figure 13. - Continued. (d) metal injected mold, (e) part removed.

the insulated cylinder, the preheated mold is clamped on top and the metal injected. The time from melting metal ingots to metal injection (figure 13d) is less than 10 minutes.

Removing the casting from the mold using a water jet (figure 13e) takes an additional 45 minutes. Clean up and hand working of the aluminum model takes only a few additional hours as the casting captures most of the surface detail and smoothness. Additional hand working may be needed only for removal of the gates and vents if the casting is successful.

Figure 14 shows aluminum X37 model castings from injected wax patterns. The castings were thin walled, which was done for two reasons. First was to improve casting precision. Solid castings have problems with heat dissipation and uneven solidification. Second, was to provide a convenient interior space for force and moment balance instrumentation. The same outer wax mold used for the X37H ceramic model was used for process development. An additional core mold was made by lining the outer mold with an eighth-inch-thick sheet of compliant wax and injecting with a second water soluble wax. Quarter-inch aluminum cubes, or "chaplets," were first fit in the lining and then left in the core mold to ensure proper alignment after the lining is removed. These chaplets later become part of the final casting. The core mold and subsequent injected wax pattern are shown in figure 15.

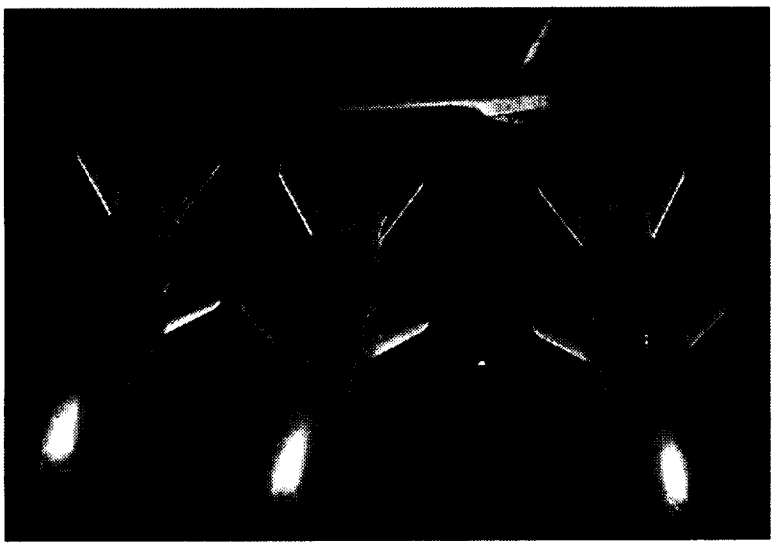

Figure 14. - Pressure cast aluminum X37H models.

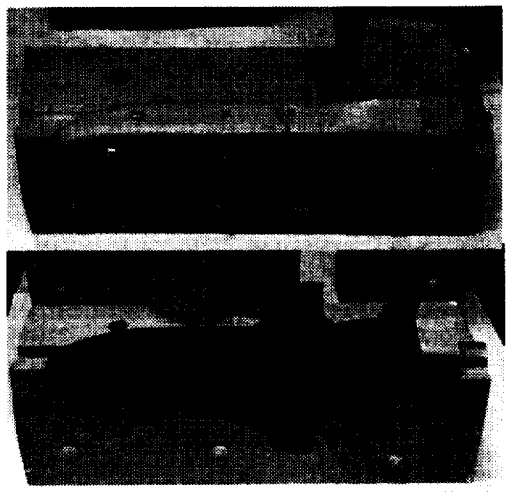

Figure 15. - Core mold (top) and injected wax pattern (bottom).

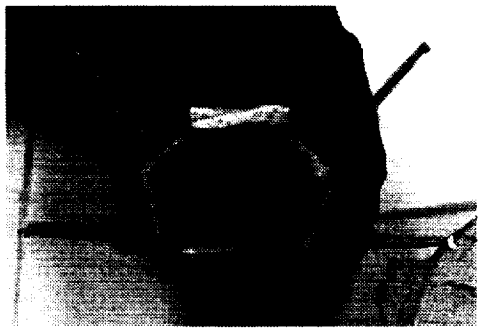

Figure 16. - Cast boss for machine fitted steel sleeve.

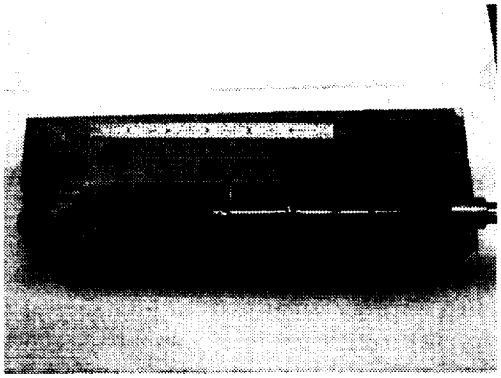

Figure 17. - Steel sleeve alignment.

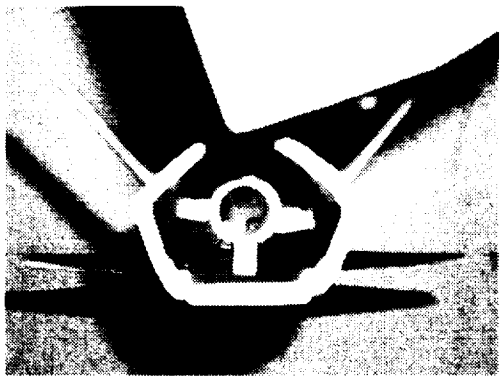

Figure 18. - Cast fitted steel insert.

For force and moment test models, both outer surface fidelity and balance alignment and positioning are important factors. Two methods were used to fit precision bore steel sleeves to cast aluminum force and moment models. The first method involved casting an internal cylinder, or "boss", to accept a machine fitted and pressed sleeve (figure 16). The second involved casting the steel sleeve in position. Figure 17 shows sleeve alignment in the outer mold before forming the core mold and figure 18 shows the resultant aluminum casting with steel balance sleeve.

Both methods require approximately the same effort and time in the casting process. The machine fitted steel insert takes extra time and effort, but may provide better control in balance alignment with this particular mold design. Both techniques are currently being evaluated.

Scan comparison data for a wax pattern and subsequent aluminum casting are shown in figures 19 and 20. The scan comparisons are shown in a gray intensity scale from ± 0.035 inches. The scanned point cloud data in figure 20 was scaled up 0.985% isotropically to account for shrinkage in the aluminum casting. Both sets of scan data were best fit to the windward surface. After scaling, the aluminum casting in figure 20 is shown to replicate the wax pattern windward surface in figure 19 to within ± 0.010 inch. On the sides of the model, the relative width of the scaled casting has increased +0.020 inches (approximately 1%), indicating shrinkage in the vertical but not horizontal casting directions. These scans and others can be used to redesign investment patterns to account for directional shrink factors in the metal casting.

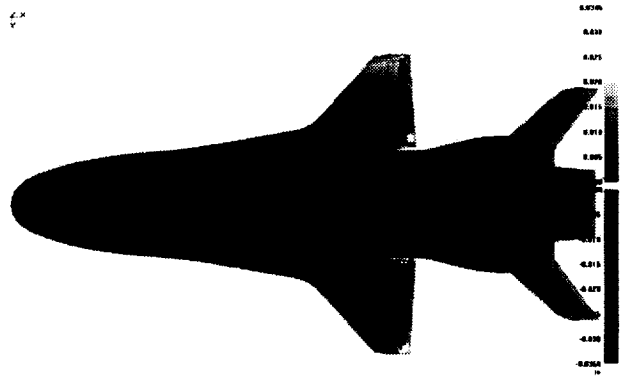

Figure 19. - Injected wax pattern, X37H.

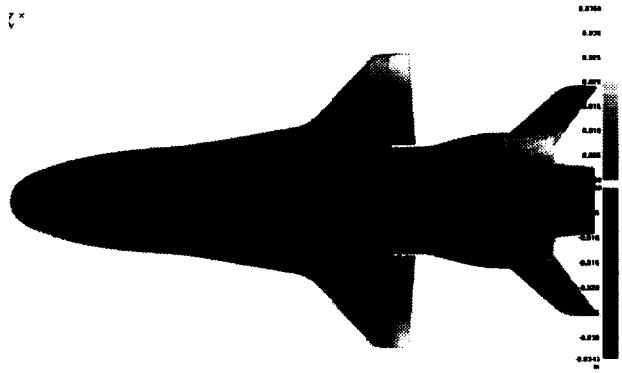

Figure 20. - Cast aluminum model, X37H.

Rapid Prototype Investment Patterns

The speed and precision for each of the investment casting techniques discussed, for ceramics and metals, is dependent on the fabrication of investment patterns. More precise investment patterns for castings have been possible for some time. Figure 21 shows a machined wax pattern used for investment slip cast molds in 1993. (See also figure 6.) Just as machining can be used to fabricate metal and ceramic models directly, precision machining of patterns can, in reality, be maintained only for relatively short periods of time and requires high Center priority, as machine space is limited and expensive.

Figure 21. - Numerically machined investment wax pattern for HL-20 test model.

Advantages in using rapid prototyping methods such as stereolithography, fused deposition or ink jet solid printers are increased production, the ability to build several components simultaneously and the ability to fabricate internal cavities. Figure 22 shows an investment pattern built using stereolithography resin with a steel sleeve inserted for force and moment balance mounting. Figures 23a, b and c show scan comparisons for the bottom, side and top of the model. For these comparisons, stereolithography investment patterns were built to within $\pm$0.010 inch tolerance. For the experience, effort and care used in producing this model, this is probably close to the maximum accuracy achievable with this method for this model size.

Stereolithography resin investment patterns are built with a thin wall honeycomb configuration to allow the pattern to collapse upon itself instead of expanding and damaging the investment mold during burnout. The problem experienced has been high residue, or "char" remains in an investment mold from the stereolithography resin, particularly in thin sections where it is not easily aspirated out from the mold later. Figure 24c shows the results of char remains on a cast surface. On this thin model, the remains of resin char have caused voids completely through the 0.020-inch thick sections.

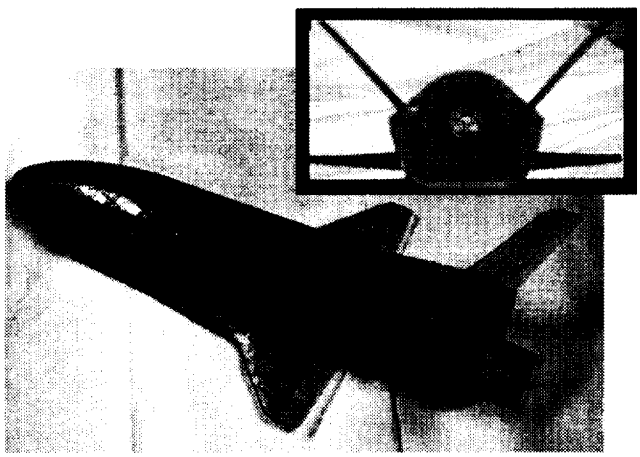

Figure 22. - Stereolithography resin thin wall Quickcast® investment pattern with steel sleeve insert for force and moment balance, X37H.

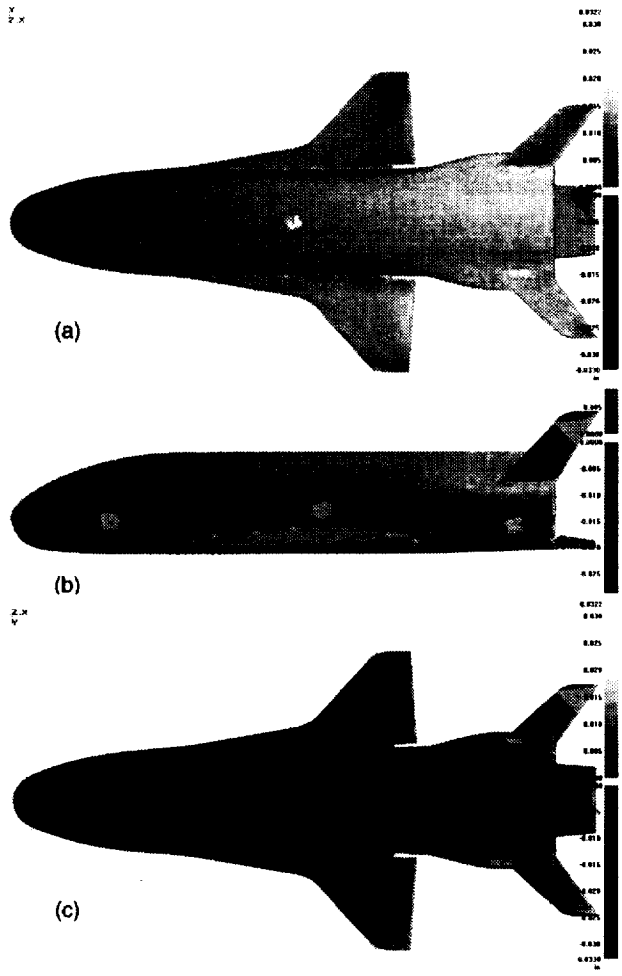

Figure 23. - Scan comparison for Quickcast® stereolithography resin invest pattern, (a) top, (b) side and (c) bottom view.

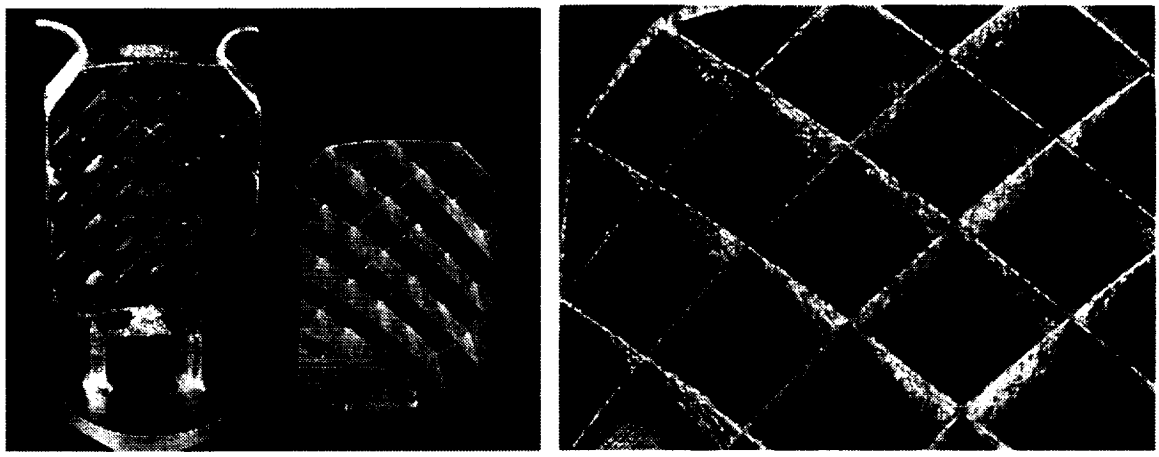

(a) (b) (c)

Figure 24. - Pressure cast aluminum model of a lattice fin control structure, (a) as cast, (b) stereolithography investment pattern, and (c) close up of model surface.

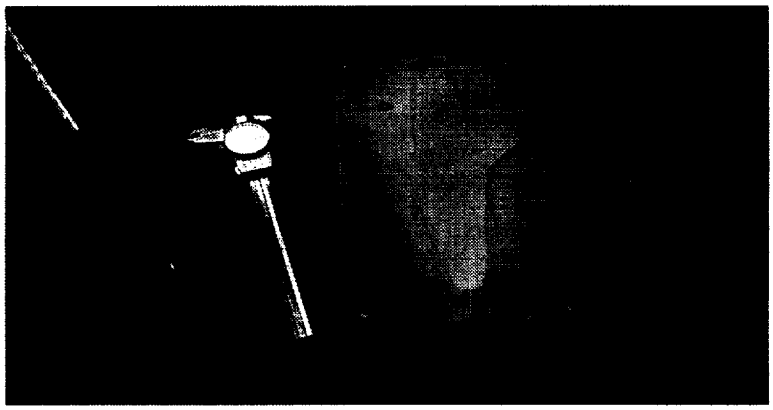

Figure 25. - Stereolithography pattern, bottom wax mold from pattern and injected wax pattern from mold.

Figure 26. - Scan comparisons for stereolithography pattern, bottom wax mold and injected wax pattern.

Two approaches are being taken with the metal pressure casting system to reduce char affects. First is to blow oxidizing gas into the mold cavity to more efficiently burn out the resin and the second is to develop higher temperature ceramic molds to burn out the char at higher temperatures. The first approach has not been successful thus far and the second approach is being worked as of this writing.

Methods have not been developed for investing the weaker slip casting shells with stereolithography resin patterns either. Even with a honeycomb build configuration, thermal expansion of the stereolithography resin cracks and damages the more delicate slip molds.

For successful castings since 1995, intermediate wax injection molds have been formed from stereolithography resin patterns and injected wax patterns from these used for investment casting. A Stereolithography pattern, mold and wax pattern are shown in figure 25.

The wax injection mold is formed on the stereolithography pattern from an epoxy plastic. Figure 26 shows scan comparisons of the resin pattern, mold and wax pattern shown in figure 25.

Scan comparisons such as these are being used to evaluate and improve the system. More accurate materials for injection molds and better methods of handling and processing injected wax patterns are being investigated.

Direct fabrication of wax investment patterns using solid wax ink jet printers is also being investigated. Two systems were installed and evaluated in 1999. One system uses two piezoelectric ink jet print heads to deposit materials onto the part being built. One print head deposits a thermoplastic polymer and the other print head deposits a support material which is chemically soluble for later removal. An integral cutting head mills off the top of the deposited wax for accuracy, and can remove additional layers in the case of a print failure to resume a build without restarting. The most advanced feature of this system is its ability to build layers of only 0.0005" in thickness and a surface finish of 32-63 micro-inches RMS. This capability is more precise than any other rapid prototyping system at this time. (Chuk and Thomson, 1998)

The first most obvious trade off with this precise solid wax printer is speed. It took 5 days to build a six-inch model horizontally, and this model was damaged by a print head failure. The system has had several mechanical failures leading to several part replacements since installation. The slow builds and the frequent breakdowns has provided only a few, small, complete parts for evaluation. These parts have been very smooth and accurate as shown in Figure 28. The build chamber is large enough for parts up to 12x6x9 inches.

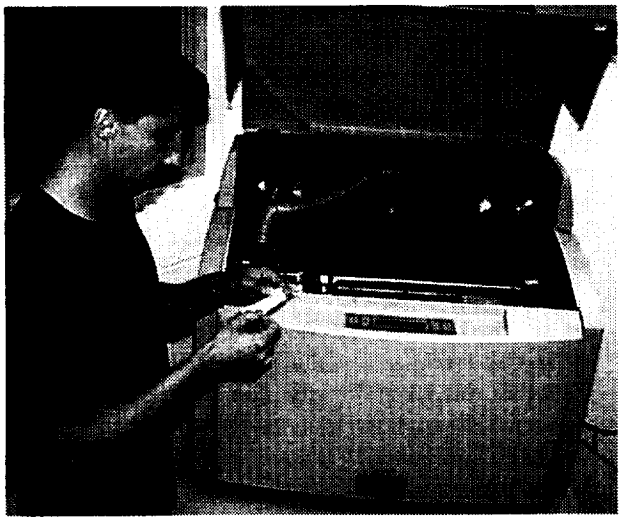

Figure 27. - Diagnosing a print head failure on the first solid wax ink jet printer system.

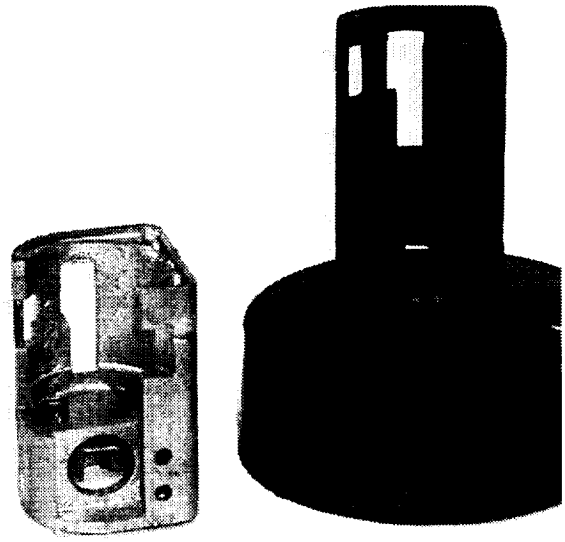

Figure 28. - 2-inch aluminum casting and printed wax component on wax gates for casting.

The second system uses 352 piezoelectric ink jet print heads to deposit material onto the part being built. All print heads deposit thermoplastic polymer. Supports resemble a fine bed of pins and are used to support overhangs and internal cavities. Support material is later scraped away from the build surface by hand. The most advanced feature of this system is its ultra high speed build capability. The high print resolution (300 dpi) produces smooth upper surfaces directly useful for casting dyes and tooling. The accuracy quoted from the manufacturer is ±0.010 inches.

The trade off with this system is the rough lower surface where the support material is scraped away. A model was built in the vertical direction (figure 29a) and required less than a day to complete. The problems were ragged edges on the thin trailing surfaces from removing support material and difficulty in removing support material up inside the model. Also, the size is more limited in the vertical build direction, as the build chamber will accommodate part sizes up to 10x7.5x8 inches, with the 7.5 inches in the vertical direction. For desired 8-inch test models, three build solutions were tested. Figure 29b shows a build configuration split lengthwise and later rejoined after support material is removed from the center. Perhaps due to uneven build in two different chamber locations these two sections had an overhang when joined together. When split in cross section (figure 29c) the model did not align straight. Finally, the model was built in one piece, with the windward surface upward and a separate hatch for removing support material (figure 29d).

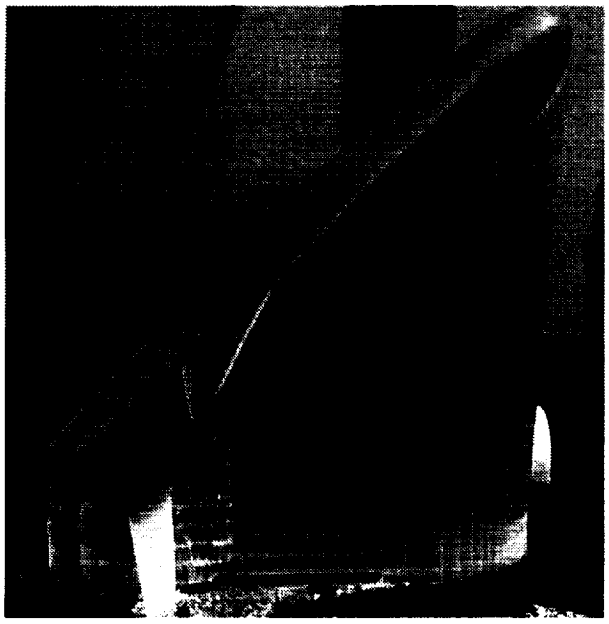

Figure 30. - Build angle at 45°.

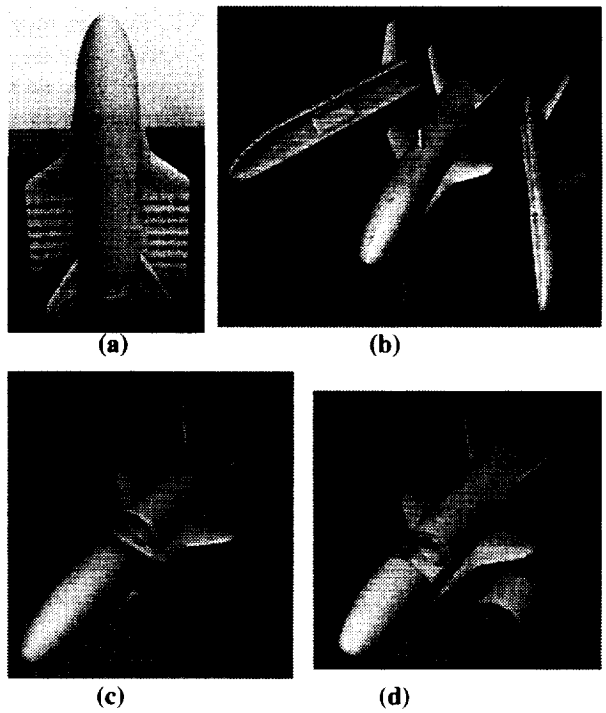

Figure 29. - Build configurations for X37H in second solid wax ink jet printer system, (a) 6-inch vertical build, (b) 8-inch lengthwise split horizontal build, (c) 8-inch split cross section build and (d) 8-inch with hatch for removal of support material.

To have continuous smooth build surfaces around the nose and leading edges of a model, a build configuration was made at an angle equal to the nominal test angle-of-attack for the vehicle. Figure 30 shows how the smooth build surfaces wrap around the nose and leading edges.

Major concerns with the second, faster solid wax printer are distortion and uneven shrinkage depending on part geometry and build direction. Figures 31 and 32 show scan comparisons for the horizontal and 45° build shown in figure 30. The elliptical center depression shown in figure 31 may be caused by insertion of a steel balance sleeve before scanning. Note the differences between the side panels beneath the tail fins and the adjacent lower or windward surface, indicating shrinkage in the y direction. The scan in figure 32 was taken directly after being built, before it was removed from the plate as shown in figure 30. In this build configuration there is a downward deflection of the body flap, tail fins and wing tips, with a similar shrinkage in the y direction as would be expected. More build tests are being made to see how repeatable the system is for a particular build configuration and if optical scan data might be used to adjust the build file to compensate for distortions and uneven shrinkage.

Examples would be to scale the model differently in different build directions, compensate for shrinkage in solid thick and thin sections, or to just customize corrections for a particular model series based on scan data without necessarily understanding the build factors.

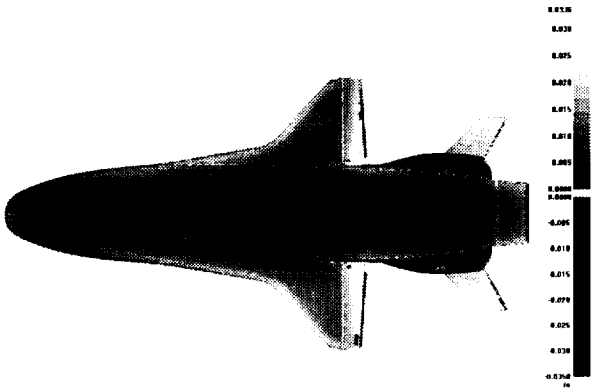

Figure 31. - Scan for horizontal build.

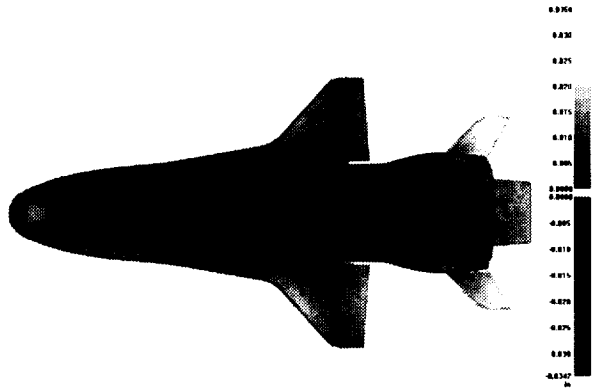

Figure 32. - Scan for build angle at 45°.

Global Pressure and Temperature Measurements

Global measurement techniques revolutionize wind tunnel testing by providing high resolution surface measurements in very little time with low cost. The impact of two-color thermographic phosphor techniques on aerothermodynamic studies at Langley has been presented. Now, similar techniques are being developed for simultaneous pressure and temperature measurements in heated hypersonic wind tunnels using three-color luminescent coatings and imaging systems.

From Paints to Dyes to Powders

Pressure-sensitive paint techniques have been developed and tested broadly by NASA centers, industries, and universities for lower-speed and lower-temperature applications. (Liu et al., 1997) Current techniques use oxygen-sensitive luminophores in polymer binders for pressure sensitive paints which can be applied to a variety of surfaces. In high-speed applications with aerodynamic heating, however, temperature affects on induced luminescence complicate pressure measurements.

A few years ago, work was done to calibrate temperature effects on the luminescence of a paint for high-speed applications (Morris and Donovan, 1994) but it was later demonstrated (Jules and Zemsch, 1995) that higher temperature significantly affects the response of this paint and that past a certain temperature threshold (40-60C) luminescence degradation becomes irreversible.

Earlier work by the author (Buck, 1995) used a ceramic-dye matrix for higher temperature (150C) simultaneous pressure and temperature measurements on small samples. Slip-cast silica ceramic was used as a porous substrate onto which a pressure sensitive compound in a dye was adsorbed. The luminophore, a perylene compound, was stable up to 320C, but evaporated from the ceramic substrate above 150C. The response was also a function of the adsorbed film thickness, which became increasingly difficult to control over large areas such as model surfaces.

Current work focuses on simultaneous pressure and temperature sensitive coatings using a composite powder formula with a pressure sensitive luminophore in a glass polymer matrix combined with ceramic phosphors for reference and temperature measurements. Continuous stable operation has been demonstrated up to 210C with even higher temperature use expected for short duration wind tunnel testing.

Two-color measurement techniques for thermographic phosphor powders have been useful (Buck, 1988, 1991 and Merski, 1999) but similar applications with pressure sensitive paints have frustrated researchers because of uneven characteristics of the painted surface, and still require wind-off and wind-on measurements to calibrate the surface variations. This method has been termed "ratio of ratios." With powders, the mixing of materials averages the variation in luminescence providing uniform surface distribution in coatings. A three-color technique is the next approach for simultaneous pressure and temperature measurements with a powder coating system.

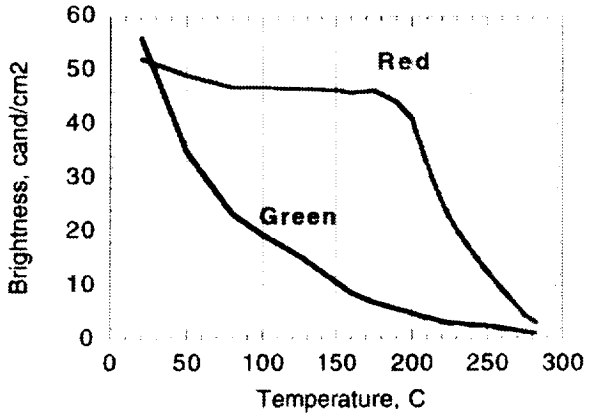

Figure 33. - Two-color thermographic phosphor coating.

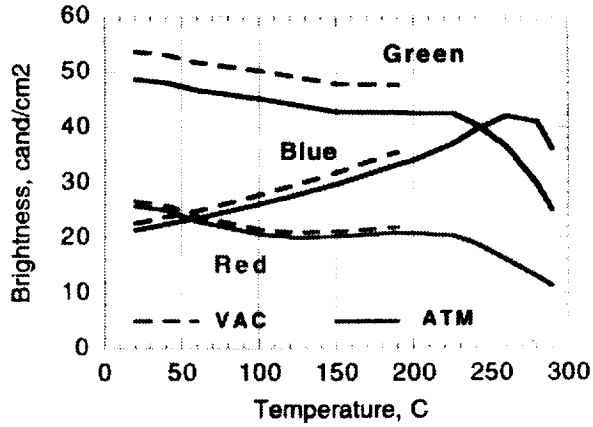

Figure 34. - Three-color pressure- and temperature sensitive powder coating.

Three Color Digital Imaging Systems

The need for higher dynamic range, or in digital terms, bit resolution is the first problem encountered with the three-color approach. The emission spectra of the various pressure, temperature and reference luminophores overlap to some degree and are multiply present in the dichroic color filtered images. After developing the first powder coating for the three-detector analog-to-digital color imaging system already in use for two-color phosphor thermography, it became apparent that a higher bit resolution was needed. Figures 33 and 34 show the imaging system response to the current two-color phosphors and three-color luminescent powder respectively. As shown in figure 33, response of the current thermographic phosphors is full scale over the temperature sensing range. For the pressure- and temperature-sensitive luminescent powder the green output is shown to be most pressure sensitive. In this system, pressure response is only 15% of full scale over the range in pressure from vacuum (~4 torr) to atmosphere.

The current analog-to-digital imaging system has at maximum an eight-bit resolution. The search for a three-detector digital color imager of higher bit resolution was unsuccessful. Single-detector digital color imagers were then evaluated to find one with an optimum color filtering scheme. A ten-bit 1300x1030 array digital color imager was selected with a 1:2:1 R-G-B filter distribution as shown in figure 35. Most other color image detectors evaluated use 1:4:1 or 1:6:1 R-G-B filtering schemes.

In developing the latest powder formula the challenge is now twofold. First is to dramatically change the original formula so that the green emission

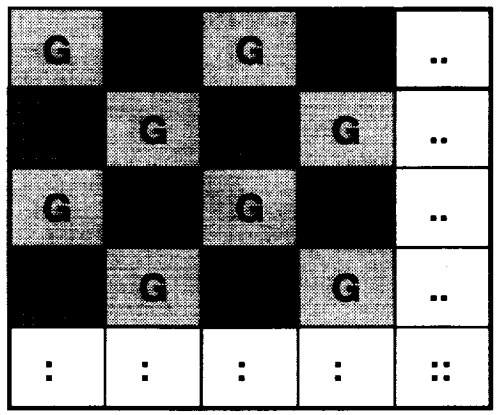

Figure 35. - Color filter pattern of single array digital color imager.

is half that of the blue and red. Second is to balance the colors more closely than before because variable color gain is not possible with the single image detector. These challenges have been met to some degree and a large enough batch of three-color luminescence simultaneous pressure- and temperature-sensitive powder is being prepared for hypersonic wind tunnel testing.

Summary

Rapid fabrication of test models and measurement techniques providing simultaneous global surface pressure and temperature distributions for aerospace vehicles in hypersonic facilities are works in progress. Significant increases in productivity and cost savings

have been demonstrated with a global aeroheating test method and rapid casting techniques. Future development of rapid and accurate casting techniques for models tested in heated hypersonic wind tunnels will use rapid prototype patterns, advanced casting techniques for metals and ceramics and an optical coordinate scanning system for casting process development and final model verification. Further development of luminescent coatings and a digital three-color imaging system will provide increased capability for hypersonic wind-tunnel testing with simultaneous global pressure and temperature measurements. Together these techniques will provide a more rapid and complete experimental aerodynamic and aerothermodynamic database for future aerospace vehicles.

Acknowledgements

The following people are gratefully acknowledged for their contributions to this work: T. Biess for machining, materials and facilities evaluations; T. Vranas for NC machining; S. Nevins and G. Wainwright for installing, programming, operating and troubleshooting rapid prototyping systems; P. Vasquez for development of patterns, molds and casting techniques for metals and ceramics; C. Rogers, T. Burns, K. Kuykendoll, P. Veneris and E. Covington for optical scanning and evaluation of injected wax, printed wax, stereolithography resin, and cast ceramic and aluminum in the form of patterns, molds and models; and P. Tucker and A. Robbins for processing, coating and testing high temperature pressure and temperature sensitive coatings.

References

Buck, G. M., "An Imaging System for Quantitative Surface Temperature Mapping Using Two-Color Thermographic Phosphors," ISA Paper 88-0772, May 1988.

Buck, G. M., and Vasquez, P., "An Investment Ceramic Slip-Casting Technique for Net-form, Precision, Detailed Casting of Ceramic Models," U.S. Patent 5,266,252, November 1989.

Buck, G. M., "Surface Temperature/Heat Transfer Measurement Using a Quantitative Phosphor Thermography System," AIAA Paper 91-0064, January 1991.

Buck, G. M., "Simultaneous Luminescence Pressure and Temperature Measurement System for Hypersonic Wind Tunnels," *Journal of Spacecraft and Rockets*, Vol. 32, No. 5, September-October 1995, pp. 791-794.

Chuk, R. N., and Thomson, V. J., "A Comparison of Rapid Prototyping Techniques Used for Wind Tunnel Model Fabrication," *Rapid Prototyping Journal*, Vol. 4, No. 4, 1998, pp. 185-196.

Dean, D. G., and Connor, L. E., "a Study for Development of Aerothermodynamic Test Model Materials and Fabrication Technique," NASA CR 2065, June 1972.

Jules, K., Carbonaro, M., and Zemsch, S., "Application of Pressure Sensitive Paint in Hypersonic Flows," NASA TM-106824, February 1995.

Liu, T., Campbell, B. T., Burns, S. P., and Sullivan, J. P., "Temperature- and Pressure-Sensitive Luminescent Paints in Aerodynamics," *Applied Mechanics Reviews*, Vol. 50, No. 4, April 1997, pp. 227-246.

Merski, N. R., "Reduction and Analysis of Phosphor Themography Data with the IHEAT Software Package," AIAA Paper 98-0712, January 1998.

Merski, N. R., "Global Aeroheating Wind-Tunnel Measurements Using Improved Two-Color Phosphor Thermography Method," *Journal of Spacecraft and Rockets*, Vol. 36, No. 2, 1999, pp. 160-170.

Miller, C. G., "Comparison of Thin-Film Resistance Heat-Transfer Gages with Thin-Skin Transient Calorimeter Gages in Conventional Hypersonic Wind Tunnels," NASA TM 83197, December 1981.

Miller, C. G., "Experimental and Predicted Heating Distributions for Biconics at Incidence in Air at Mach 10," NASA TP 2334, November 1984.

Miller, C. G., "Aerothermodynamic Flight Simulation Capabilities for Aerospace Vehicles," AIAA Paper 98-2600, June 1998.

Morris, M. J., and Donovan, J. F., "Application of Pressure- and Temperature-Sensitive Paints to High-Speed flows," AIAA Paper 94-2231, June 1994.

Schultz, D. L., and Jones, T. V., "Heat-Transfer Measurements in Short-Duration Hypersonic Facilities," AGARD Report AG165, 1973.

Springer, A., "Evaluating Aerodynamic Characteristics of Wind-Tunnel Models Produced by Rapid Prototyping Methods," *Journal of Spacecraft and Rockets*, Vol. 35, No. 6, 1998, pp. 755-759.

Vasquez, P., Hutto, W. R., and Philips, A. R., "Pressure Rig for Repetitive Casting," U.S. Patent 4,865,114, September 1989.